TECHNICAL NOTES

NATIONAL ADVISORY COMMITTEE FOR AERONAUTICS

No. 683

PRESSURE-DISTRIBUTION MEASUREMENTS ON A TAPERED WING WITH A FULL-SPAN SPLIT FLAP IN CURVED FLIGHT

By Th. Troller and F. Rokus
Daniel Guggenheim Airship Institute

Washington
January 1939

NATIONAL ADVISORY COMMITTEE FOR AERONAUTICS

TECHNICAL NOTE NO. 683

PRESSURE-DISTRIBUTION MEASUREMENTS ON A TAPERED WING WITH A FULL-SPAN SPLIT FLAP IN CURVED FLIGHT

By Th. Troller and F. Rokus

SUMMARY

Pressure-distribution tests were made on the 32-foot whirling arm of the Daniel Guggenheim Airship Institute of a tapered wing to determine the rolling and yawing moments due to an angular velocity in yaw. The model was tested at 0° and 5° pitch, -1° and 5° yaw, and with a full-span flap deflected 60°. The results are given in the form of span load distributions and in calculated moment coefficients. The rolling-moment coefficients are in fairly close agreement with those derived by means of a simple approximative theory even for high deflection of the full-span flap.

INTRODUCTION

An investigation of the pressure distribution over a tapered wing model, with a full-span split flap while in curved flight, was made on the 32-foot whirling arm in order to obtain the aerodynamic moments for such a flight condition. The following wing positions were investigated: model at 0° and 5° pitch, each with -1° yaw and 0° and 60° flap deflections; model at 0° and 5° pitch, each with 5° yaw and 0° and 60° flap deflections. Between 200 and 400 pressure points distributed over 12 chords along the span were measured for each wing position. For these tests the b/R ratio (span to turning radius) was equal to 0.133.

APPARATUS

The wing model used in these tests was built up from several sections of magnesium, which were bolted together, machined to the correct size and shape, and then filed to

a smooth finish. Owing to the limited size of the suspension tube, only 35 points could be measured at one time. The wing was therefore made hollow with the lower surface removable so that the rubber tubes connecting the pressure orifices to the measuring manometer could be changed to different positions at the end of each test run. The wing model was tapered 2:1 with the 30-percent-chord points on a straight line and the maximum ordinates of all sections in a horizontal plane on the upper surface. The wing model had a Clark Y profile, a maximum chord length of 8.91 inches, and a span of 50.45 inches (fig. 1).

The flaps used for these tests were tapered so that the chord of the flap at any longitudinal section was 25 percent of the wing chord at the same section. They were made of 1/16-inch steel plate and were hinged to the wing. The flaps, when deflected, were held in position by several small rods between the flaps and the wing at their extreme ends (fig. 2). Pressure orifices were installed on only the outer surface of the flaps. For the 0° flap condition, the flap was entirely removed and the lower surface of the wing was smoothed with wax.

The inverted wing model was attached to the whirling arm (reference 1) as shown in figures 1, 2, and 3. The small streamline tube attached to the center of the wing has a 2-inch chord and a maximum thickness of 0.75 inch. Through this streamline tube, 35 pressure tubes were led, connecting the various pressure orifices on the wing to the multiple manometer located on the central shaft of the whirling arm. Here the manometer tubes turned with the shaft at a radius of 8.25 inches. Light-sensitive paper was inserted between the manometer tubes and the shaft and was exposed to the light of four Photoflood bulbs during the test runs. A record of the heights of the meniscuses of the alcohol in the manometer tubes was thus obtained.

For these tests it was necessary to reduce the swirl in the whirling-arm channel (reference 1) even more than had been done for previous whirling-arm tests. In order to reduce the swirl, the three screen baffles, which are placed across the whirling-arm channel approximately 120° apart and which had been used to reduce the swirl for previous tests, were entirely covered with heavy wrapping paper. A rectangular opening of approximately 20 square feet was cut in these solid baffles for the wing model to pass through. This opening was of sufficient size to avoid interference with the air flow about the wing.

The pressures on the wing were measured by recording the pressure from 35 points at a time. Between each test run, the rubber tubes connecting the pressure orifices to the manometer were changed until the whole surface of the model had been surveyed.

Each record was obtained by accelerating the model slowly up to full speed and exposing the sensitized paper for about 2-1/2 minutes after the model had steadied itself at the test speed of 45 r.p.m. The photographic manometer records were taken on "ozalid" paper, a paper of low light sensitivity that is developed, after exposure, in ammonia fumes. Inasmuch as the paper is not brought into contact with moisture, no shrinkage or warping occurs.

Several tubes on the multiple manometer were opened directly to the atmosphere to be used as zero reference points. In order to obtain the absolute pressure at any point, a centrifugal-force correction, due to the length of the column of air from the manometer tubes to the pressure orifices turning with the arm, had to be added to the readings. This correction can be calculated very accurately. It is equal to the velocity head of the turning speed of the individual orifice except for the negligible value of an air column from the center of the shaft to the manometer.

In order to obtain the flight speed of the model, that is, the speed against the air, a correction had to be made for the swirl due to the motion of the arm. A hot-wire unit, suitable for measurement of the small fluctuating velocity and its direction, was used for the investigation of the swirl. Many points within the channel were surveyed and the average swirl velocity, with the model of the tapered wing attached to the arm, was found to be 0.8 meter per second. This value is 1.36 percent of the model velocity. The swirl-velocity components normal to the flight direction were found to be so small as to have practically no effect on the pitch and the yaw angles of the airfoil. The following table gives values for the swirl velocity and the effective angular change of the airfoil for three points within the channel just below the wing.

Position below airfoil	Swirl velocity (meters/sec)	Angular change due to swirl	
		Pitch (deg.)	Yaw (deg.)
6 inches below:			
inner tip	1.0	-0.05	-0.03
center	.8	0	0
outer tip	.7	.07	.07

The angular change of pitch and yaw due to the swirl component is obtained from

$$\Delta\alpha = \sin^{-1} \frac{v \sin \alpha}{V}$$

where v, is average swirl velocity, as measured on the oscillogram.

α, average angle of pitch or yaw of the swirl velocity, as measured on the oscillogram.

V, model velocity, 44.5 meters per second.

Figure 3 shows a photograph of the hot-wire mounting used in making the swirl measurements and figure 4 shows three typical oscillograms of swirl velocity, pitch, and yaw obtained for one of the positions investigated.

The velocity of the wing used throughout the computations in this report was taken as the velocity of a point at the intersection of the center line of the span and a line passing through the 30-percent point of the wing chord. This velocity was found to be 44.5 meters per second, after deducting the swirl velocity, and was used in determination of q_o, which was used for the P/q_o computations.

TEST RESULTS

Typical diagrams of the pressure distributions over the upper and lower surfaces of the airfoil and the flap are given in figure 5 as ratios of the static pressure P

to the dynamic pressure q_o of the true flight velocity.

The pressure diagrams for the various wing positions were graphically integrated and from the data thus obtained nondimensional coefficients were computed for the wing as a whole.

The local normal-force coefficient c_n and the local chord-force coefficient c_c are plotted in the load grading curves of figure 6,

where $$c_n = \frac{n}{q_o \, c_{local}}$$

$$c_c = \frac{c}{q_o \, c_{local}}$$

In figure 7 are given the rolling-moment coefficient C_l and the yawing-moment coefficient C_n obtained by graphical integration $\int_{-b/2}^{b/2} Fydy$

where $$C_l = \frac{L}{q_o \, b \, S}$$

$$C_n = \frac{N}{q_o \, b \, S}$$

and n, normal force per unit span along longitudinal axis of wing.

c, longitudinal force per unit span.

c_{local}, chord of airfoil section.

S, total wing area.

b, wing span.

y, distance along span.

Figure 7 also gives a comparison of the experimental rolling-moment coefficients with those obtained from Wieselsberger's theory for an elliptical wing in curved flight at 0° yaw. (See reference 2.) These values of

c_l are based on the theoretical moments obtained from the expression

$$L_{theor} = \frac{L_w b^2 (\beta + 1)}{16R}$$

where L_w is total lift taken from the tests.

b, span of the wing, 1.284 meters.

R, turning radius of center of wing, 9.59 meters.

β, curved vortex induction factor, 0.73 (reference 2).

The theoretical values are those of an elliptical wing of a very similar load grading in straight flight to that of the half-tapered wing used in this test.

Figure 8 shows a comparison of the theoretical load distribution along the span of the wing with the experimental points as obtained for the -1° yaw and 5° pitch wing position (negative yaw denotes turning of wing so that outer tip is moved rearward).

The theoretical curved flight load distribution was computed from the straight-flight gradient for a tapered wing (reference 3) by multiplying each sectional value by $\left(1 + \frac{y}{R}\right)\left(\frac{1 + \beta y}{R}\right)$ where y is the distance of the section from the center of the wing.

The following table gives a résumé of the resultant rolling- and yawing-moment coefficients and the ratios of $L/L_w b$ and N/Db for all the wing positions investigated in this test, where D is wing drag.

Wing condition		Flap deflection (deg.)	Coefficients		Ratios	
Yaw (deg.)	Pitch (deg.)		C_l	C_n	$L/L_w b$	N/Db
-1	0	0	0.0076	0.00033	0.00199	0.0299
		60	.0229	.00514	.00158	.0207
-1	5	0	.0136	.00073	.00166	.0290
		60	.0282	.00693	.00154	.0241
5	0	0	.0073	.00033	.00199	.0299
		60	.0225	.00832	.00162	.0339
5	5	0	.0131	.00073	.00166	.0290
		60	.0279	.01029	.00156	.0359

CONCLUSIONS

1. The rolling-moment coefficients measured at the whirling arm are in fairly close agreement with those derived by means of a simple approximative theory even for high deflection of the full-span flap.

2. The rolling moments are little affected by the angle of yaw within the range of the tests.

3. The ratio $L/L_w b$ decreases with the lowering of the flap by about 16 percent for the 0° pitch setting of the wing and is almost constant at 5° pitch.

4. The ratio N/Db decreases with the lowering of the flap.

Daniel Guggenheim Airship Institute,
Akron, Ohio, November 1938.

REFERENCES

1. Troller, Th.: The New Whirling Arm. Jour. Aero. Sci., vol. 1, no. 4, Oct. 1934, pp. 195-197.

2. Wieselsberger, C.: Zur Theorie des Tragflügels bei gekrümmter Flugbahn. Z.f.a.M.M., Bd. 2, Heft. 5, Oct. 1922, S. 325-340.

3. Glauert, H.: The Elements of Aerofoil and Airscrew Theory. Cambridge University Press, 1926, p. 155.

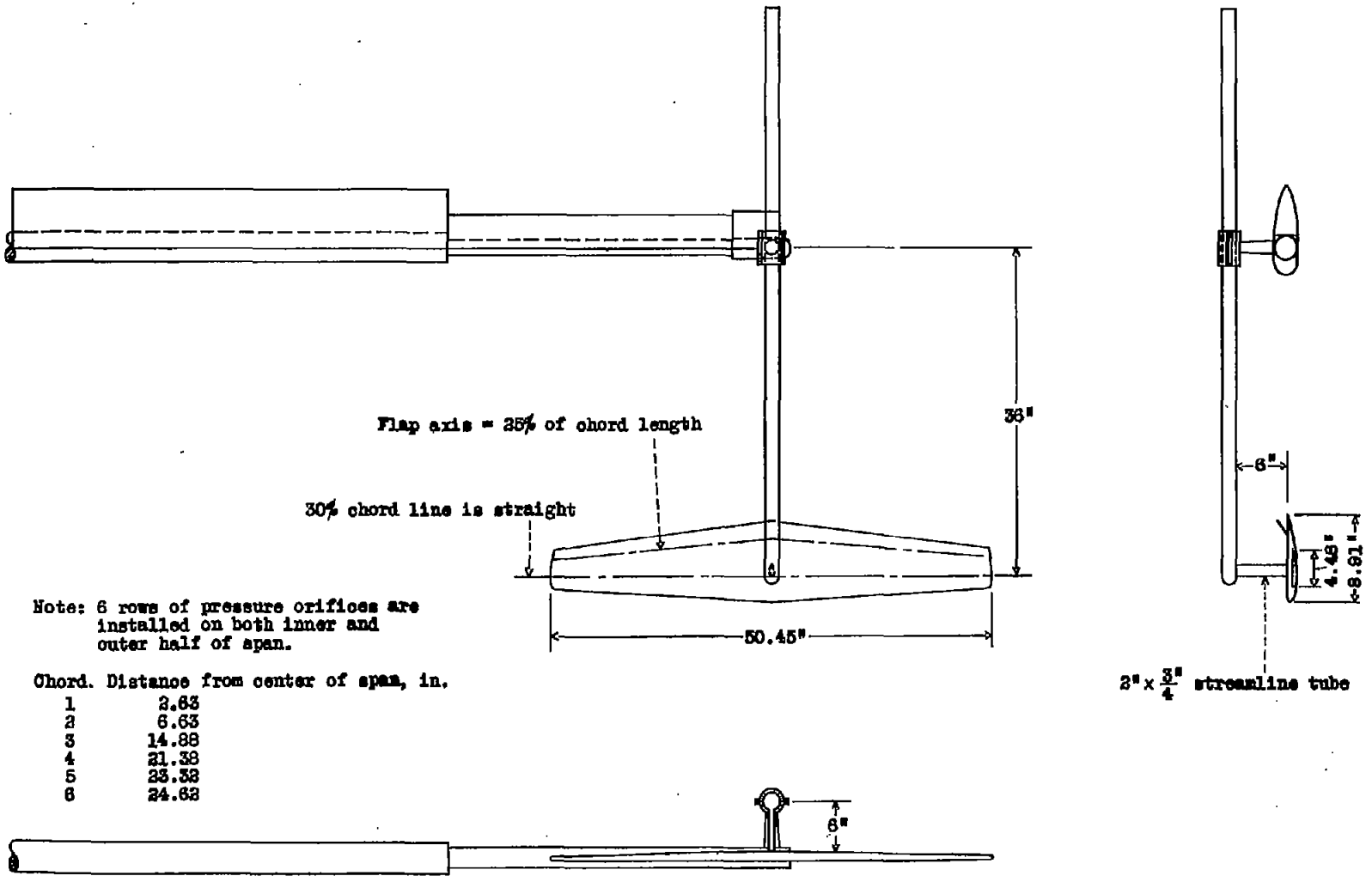

Note: 6 rows of pressure orifices are installed on both inner and outer half of span.

Chord.	Distance from center of span, in.
1	2.63
2	6.63
3	14.88
4	21.38
5	23.38
6	24.63

Figure 1.- Diagrammatic drawing showing inverted wing suspended on end of whirling arm.

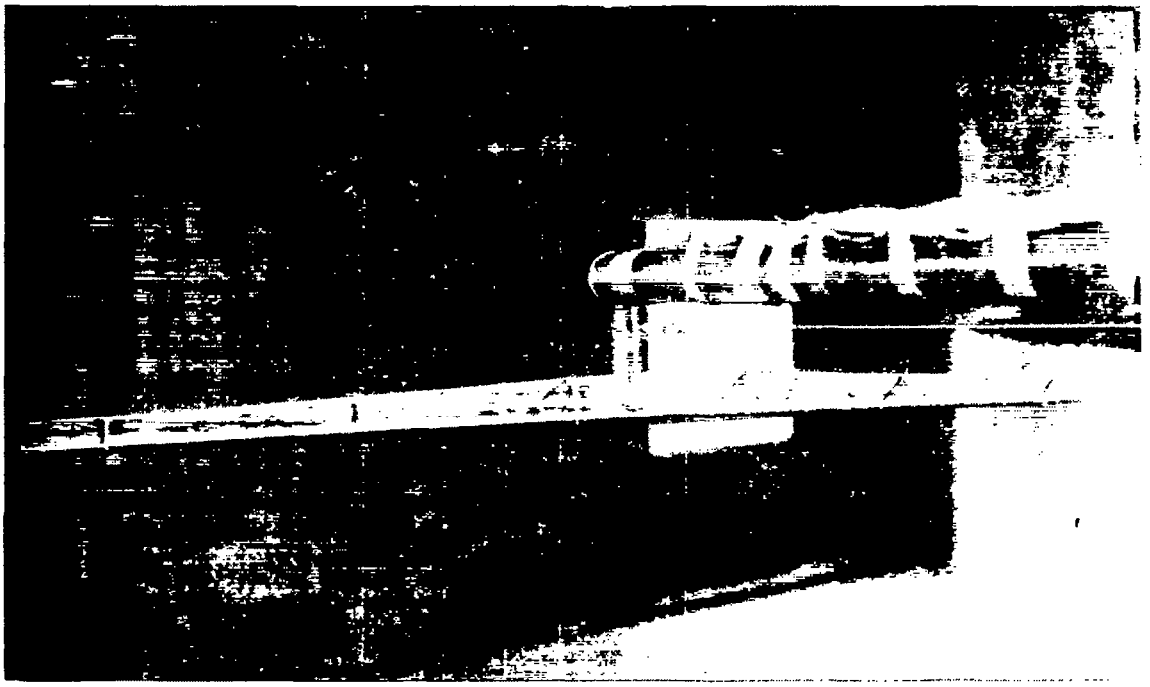

Figure 2.- Photograph of trailing edge of wing showing flap deflected.

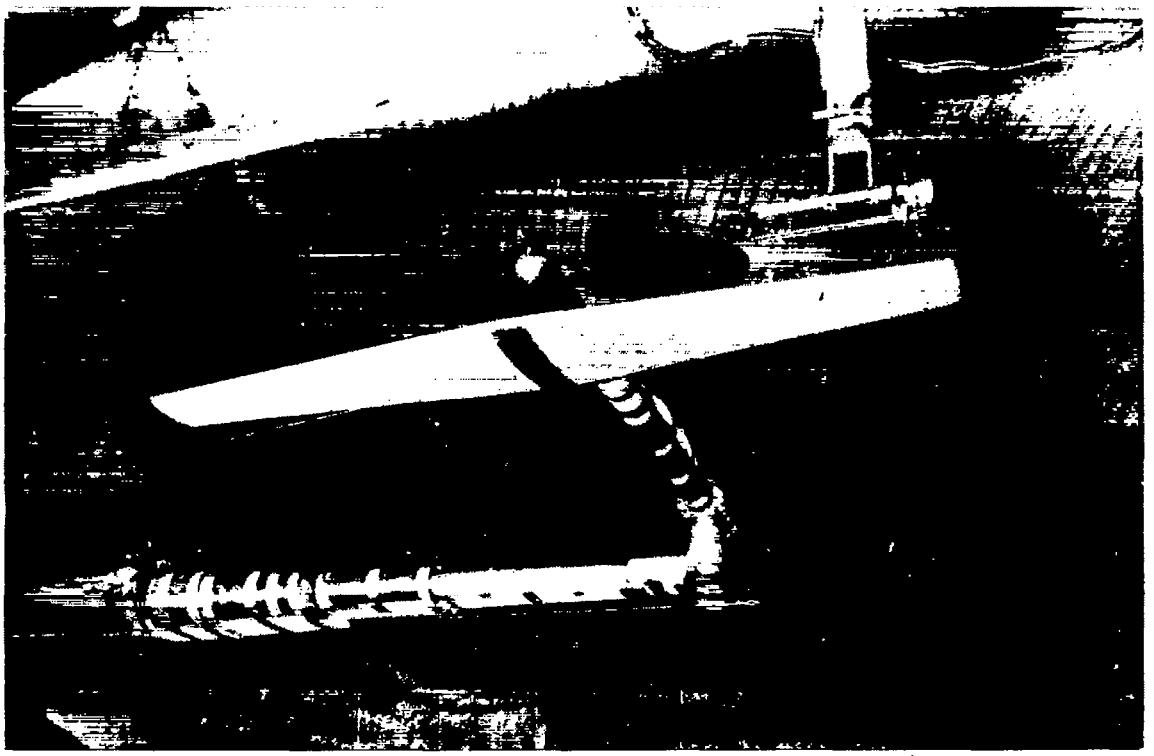

Figure 3.- Photograph of wing on end of whirling arm, showing hot-wire mounting used for making swirl measurements in whirling-arm channel.

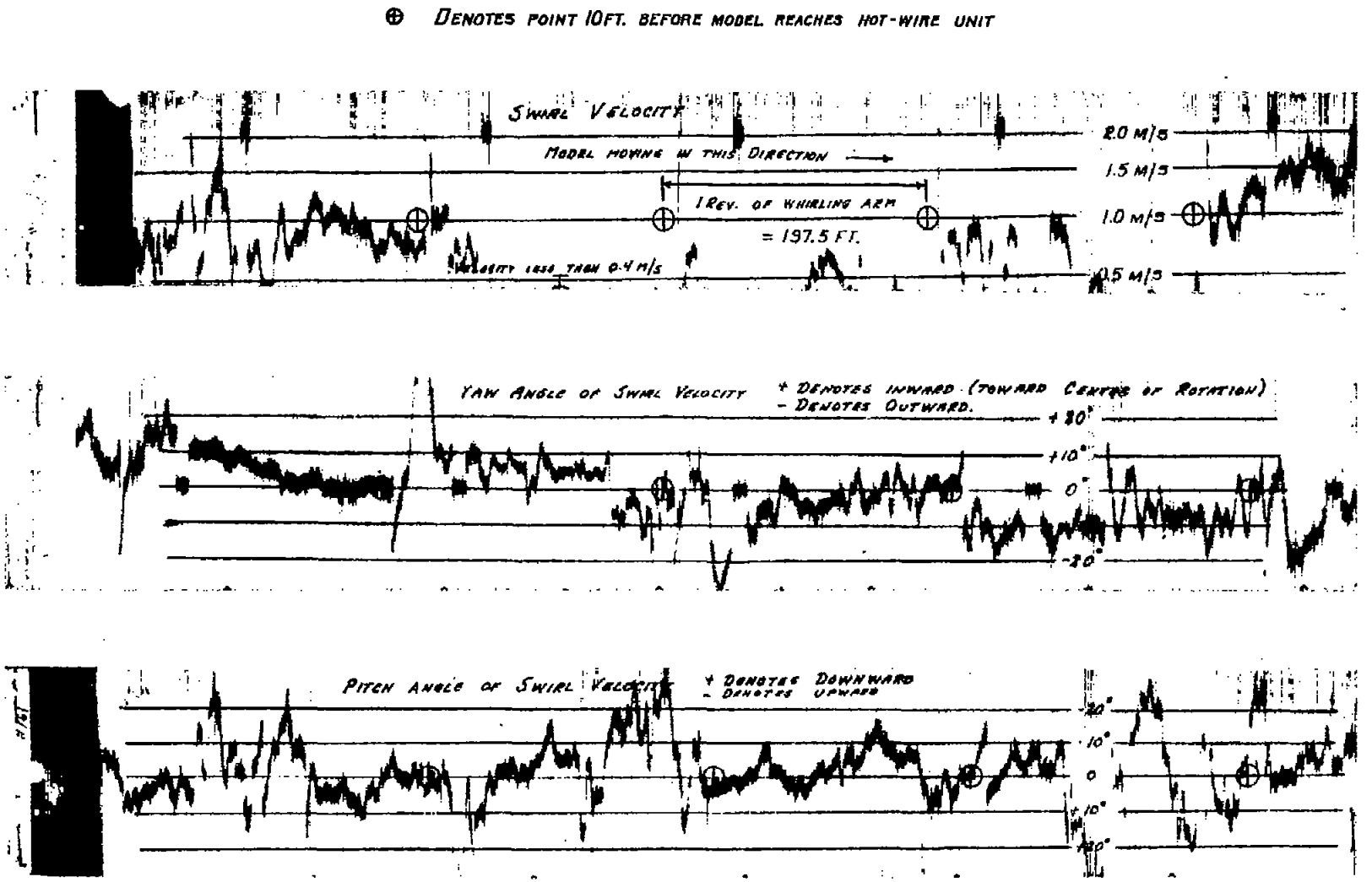

Figure 4.- Typical swirl-measurement oscillograms.

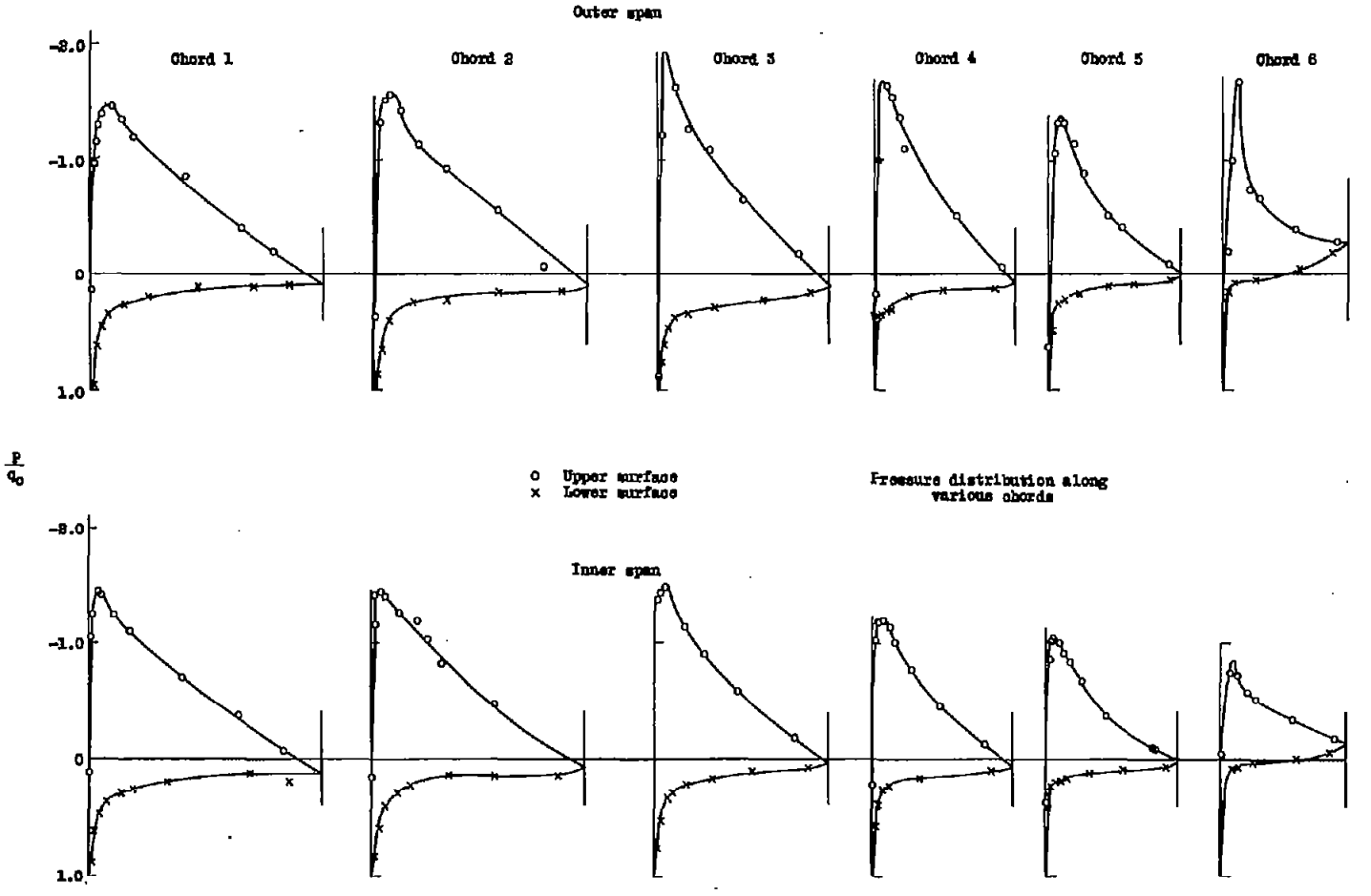

Figure 6a.- Typical pressure-distribution curves for 5° pitch, -1° yaw, 0° flap deflection.

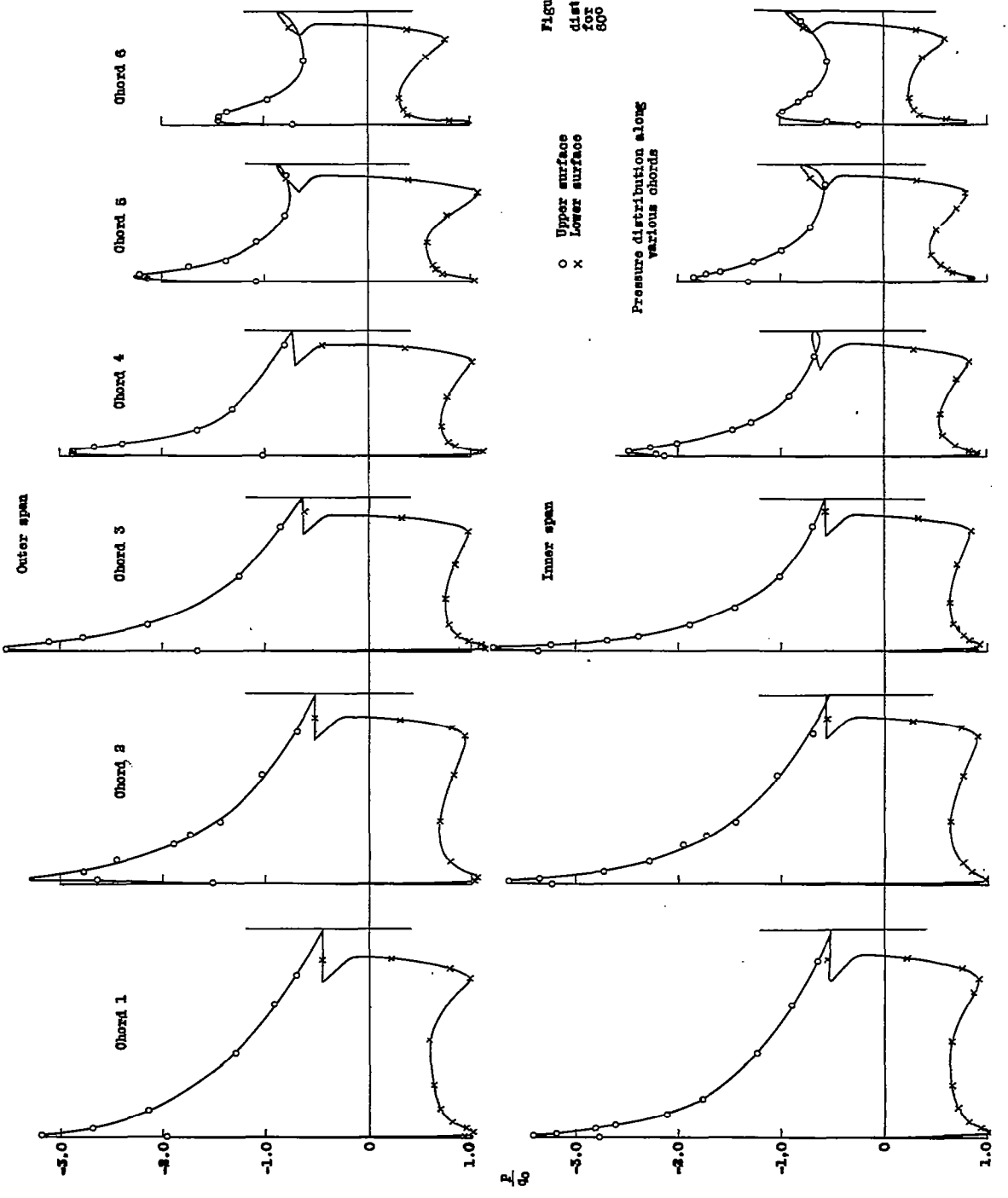

Figure 5b.- Typical pressure-distribution curves for 5° pitch, -10 yaw, 60° flap deflection.

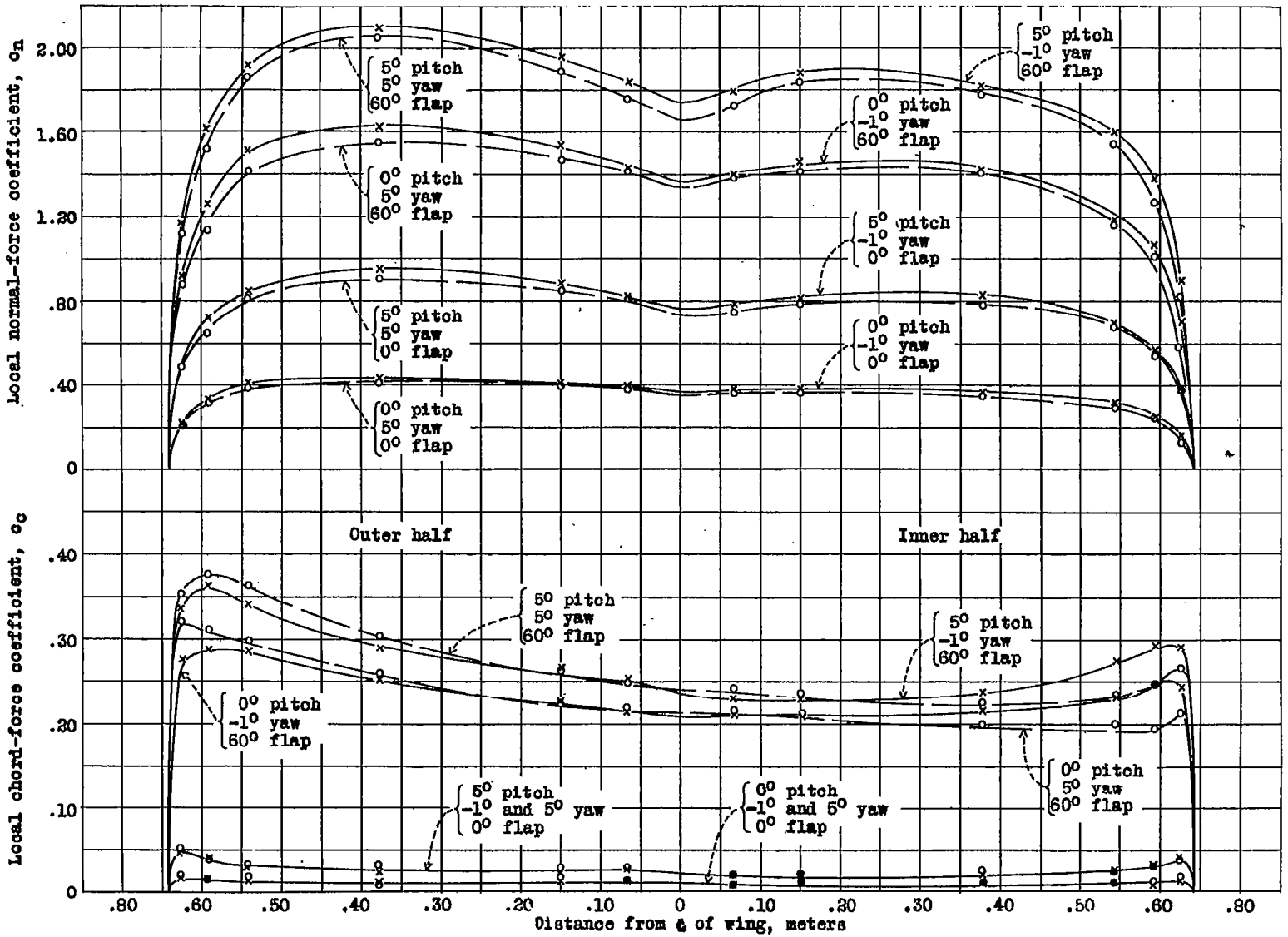

Figure 6.- Distribution of normal-force coefficients and longitudinal-force coefficients along span of wing.

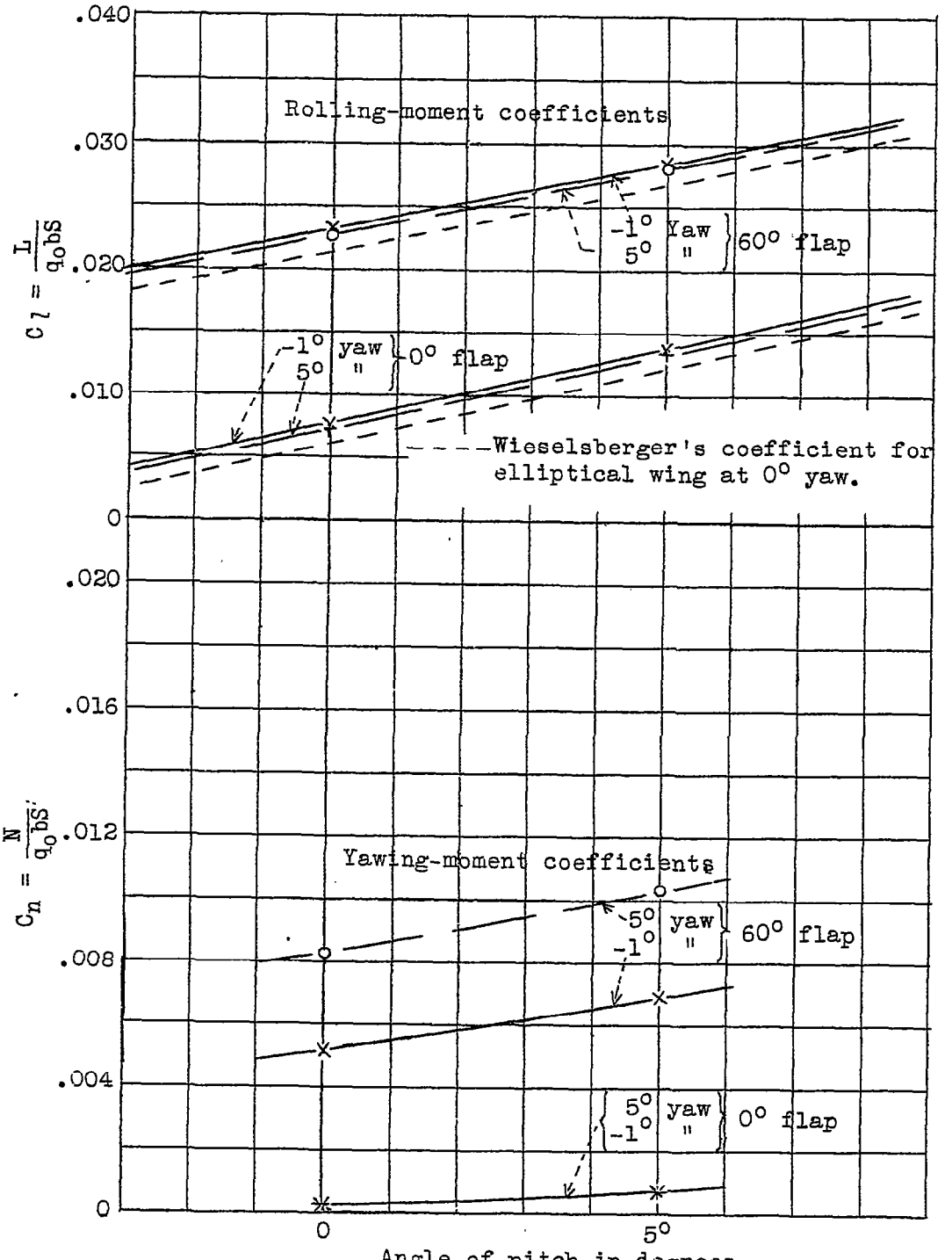

Figure 7.- Rolling-and yawing-moment coefficients.

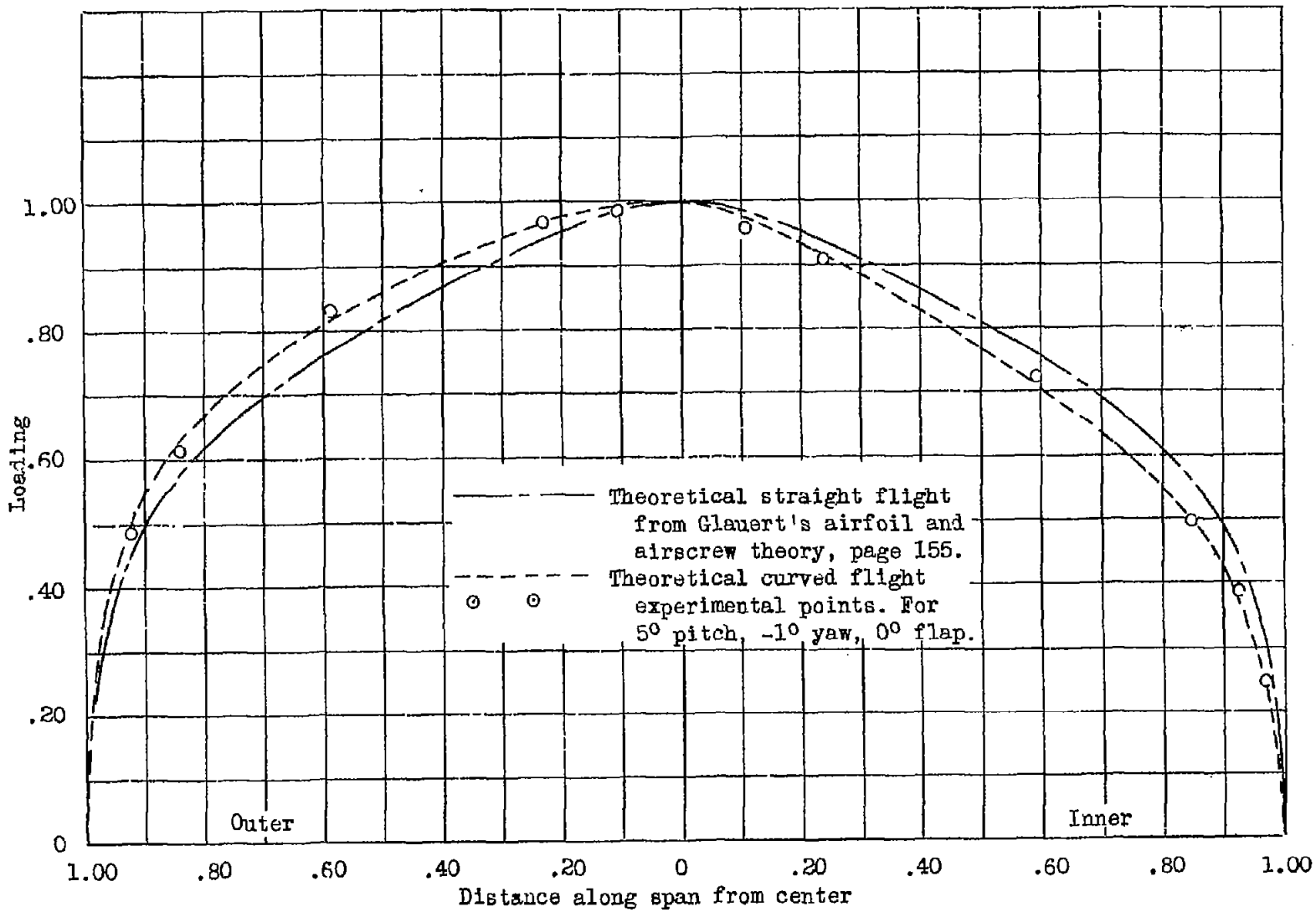

Figure 8.- Comparison of theoretical and experimental load distribution along span of wing.